Quart. J. R. Met. Soc. (1985), **111**, pp. 225–242 551.515.81

A numerical and analytical study of atmospheric undular bores

By NORMAN A. CROOK and MARTIN J. MILLER*
The Atmospheric Physics Group, Imperial College, London

(Received 11 April 1984; revised 3 October 1984)

SUMMARY

In this paper the formation and structure of an atmospheric undular bore is examined with the aid of a numerical model and theoretical analysis. The numerical model is first used to simulate a density current propagating into an unstratified environment. A detailed comparison of the model results with existing theory shows that for a given pressure head the current can travel at a greater speed than that predicted by irrotational theory.

When the density current is allowed to propagate into a low-level stable layer it is found that for certain parameter regimes an undular bore forms ahead of the current. The results for two different types of stable layers are examined. For a layer with a step profile of potential temperature, comparison is made with both classical bore theory and the theory of density currents in two-layer fluids and encouraging agreement is found. When a linear profile is specified in the stable layer it is found that energy-conserving solutions can be obtained. The numerical fields are then compared with measurements of the morning glory, an undular bore observed in north-eastern Australia, and again agreement is good.

Finally, preliminary results of model simulations with stratification above the stable layer are discussed.

1. INTRODUCTION

In the past few years there has been an increasing interest in a class of phenomena broadly described as atmospheric undular bores. Examples of this phenomenon are listed in Smith *et al.* (1982), the best documented being the 'morning glory' of north-eastern Australia. Common features are an oscillation in wind velocity and pressure and, most importantly, an increase in surface pressure of the order of 1 mb after the passage of the disturbance. Most occurrences of the morning glory have had associated cloud bands; however, examples of cloud-free glorys have been reported. In other examples of undular bores, for instance those reported by Kirk (1961) and Shreffler and Binkowski (1981), the presence of cloud has not been verified.

The following discussion will chiefly be concerned with the formation and structure of the morning glory as this is at present the best documented example of an atmospheric undular bore. At the time of writing three mechanisms for the initiation of the morning glory have been suggested in the literature. Clarke (1972) suggested that the morning glory forms on the katabatic flow on the western side of a line of hills on Cape York Peninsula, the position of formation being the discontinuity of slope between the hillside and the plains further to the west. This suggestion was largely ruled out as the primary method of formation in the later paper by Clarke *et al.* (1981). In that paper a second hypothesis was put forward, that the sea breeze of the previous day from the east coast of Australia excites a disturbance when it meets the low-level nocturnal or maritime inversion over the Gulf of Carpentaria and surrounding area.

A third hypothesis, put forward by Smith *et al.* (1982) to explain the glorys that move from the south, is that the same nocturnal/maritime inversion could be disturbed by a mesoscale front moving across Australia.

The second and third suggestions are essentially equivalent, the difference being only one of scale. In one case colder fluid in the form of a sea breeze disturbs the stable layer, in the other the colder fluid is associated with a mesoscale front. That an intrusion of colder, denser, fluid into a stable layer can create undular-bore-type disturbances has been shown in laboratory experiments (Maxworthy 1980; Smith *et al.* 1982; Simpson

* Present address: ECMWF, Shinfield Park, Reading.

1982). In the experiments of Smith *et al.* a long horizontal channel was filled with a thin layer of saline (density 1% greater than pure water) and then with a much deeper layer of pure water. Fluid of even greater density than that in the lower layer was then pumped at a constant rate into this two-layer system, the fluid propagating along the bottom of the tank in the form of a density current. After a certain time, depending on the pumping rate and density differences, a wave on the interface of the two-layer system would form above the current's head and then move ahead of the current. This process continued until about 3 or 4 waves had moved ahead of the current.

These laboratory experiments, although effectively demonstrating a generation mechanism, did not lend themselves easily to quantitative measurements. In the present study a similar system is studied with the aid of a numerical model and a detailed analysis is carried out on the strength and velocity of the bores produced.

2. The numerical model

The numerical model used is a two-dimensional, non-hydrostatic, primitive equation model with pressure as a vertical coordinate. The model is based on that described in Miller and Pearce (1974) with the later modifications detailed in Moncrieff and Miller (1976) and Miller and Thorpe (1981). In the present study some additional changes to facilitate the modelling of a density current are made and these are described below.

To simulate a density current in the model an inflow of cold air is specified at one end of the domain. The inflow is built up from rest over a period of approximately 60 timesteps (see section 3(*a*)) according to a hyperbolic tangent function. At the end of this initial build up period the inflow velocity $U_I(p)$ and the potential temperature deviation $\theta_I'(p)$ from a reference neutral state are of the form

$$U_I(p) = \tilde{U}(p - p_I)/\Delta p_I \qquad \theta_I'(p) = 2\tilde{\theta}'(p - p_I)/\Delta p_I \tag{1}$$

where Δp_I is the pressure difference across the inflow and p_I is the pressure at the top of the inflow. As the density current tends to exhibit linear profiles of velocity and potential temperature in the domain, similar profiles are specified at inflow. As a further device for producing smooth inflow fields the velocity at the bottom of the inflow, $\tilde{U}$, and the average potential temperature, $\tilde{\theta}'$, are linked by the equation

$$\tilde{U}^2 = Kg(\tilde{\theta}'/\theta_0)(\Delta p_I/g\rho_0) \tag{2}$$

where θ_0 and ρ_0 are surface values of potential temperature and density respectively. A value of K of approximately 1 was found to produce the smoothest fields at the inflow boundary.

On the remainder of the lateral boundaries radiation conditions are specified as described in Miller and Thorpe (1981) with one important exception. At each timestep a correction to the height field at one end of the domain is made so as to keep the vertically integrated horizontal velocity constant. If this correction is not made then the integrated horizontal velocity tends to increase monotonically until all the fluid in the domain is flowing in the same direction as the density current. Since the model has impervious upper and lower surfaces this means that the fluid far upstream has acquired a finite velocity which is clearly incorrect in a model started from rest. A further discussion of this problem and an analytic form for the correction is given in appendix A.

On the upper and lower pressure surfaces $\omega = Dp/Dt$ is assumed to vanish. Thus, air cannot flow through the top and bottom surfaces of the domain. As pressure surfaces in the system under study only vary by a few metres in the horizontal, the assumption

is a representation, albeit approximate, of rigid impervious upper and lower surfaces. The validity of this assumption has been tested by analysing, theoretically, the flow through an undular bore in both pressure coordinates (with $\omega = 0$ on the top and bottom pressure surfaces) and in height coordinates (with the vertical velocity vanishing at top and bottom). The theoretical prediction for the speed of the bore is the same in both systems as long as the potential temperature (or density) deviations are small (see Crook 1984).

To parametrize turbulence, a simple Laplacian operator is used on the fields of velocity and potential temperature. The numerical results were found to be only weakly dependent on the size of the mixing coefficients. (For example, doubling the mixing coefficients resulted in a 2% reduction in the speed of the density current.)

The stable layer is developed in the model by applying a cooling function to the lower layers of the domain. To allow the density current time to develop and move well into the domain the cooling function is not applied until after the initial build-up of the inflow. The stable layer is then formed just ahead of the approaching density current.

Two potential temperature profiles in the stable layer will be used.

(1) A step profile in which the potential temperature deviation is a constant θ'' throughout. The results from these simulations will be compared with the analytic theory developed in Crook (1983).

(2) A linear profile of the form $\theta'(p) = 2\theta''(p - p_L)/\Delta p_L$ where p_L is the pressure at the top of the stable layer and Δp_L is the pressure difference across it. These simulations will be compared with observations of the morning glory on 4 October 1979 (Clarke *et al.* 1981). For simplicity the fluid above the lower layer is neutrally stratified in both cases. A definition sketch showing the density current and the stable layer and the notation to be used is given in Fig. 1.

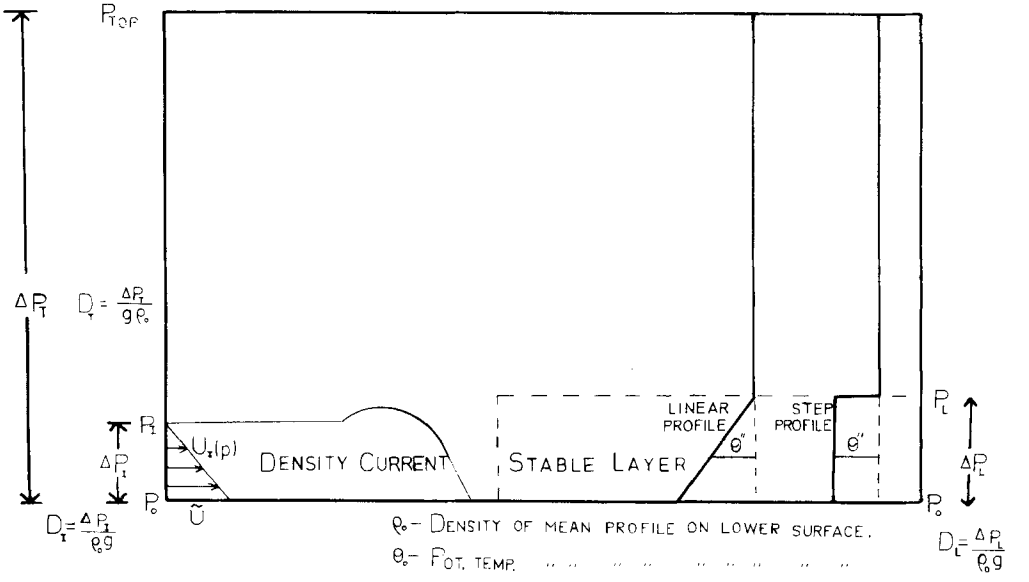

Figure 1. Definition sketch of density current and stable layer showing the notation to be used. The two profiles of potential temperature in the stable layer are also depicted.

To present the results from the numerical simulation and to simplify the analysis it is convenient to non-dimensionalize the fields. This requires that relevant dimensional scales be chosen. For the pure density current simulation the most suitable scales are:

(1) pressure scale $P_S = \Delta p_I$, pressure difference across inflow
height scale $H_S = \Delta p_I/\rho_0 g$, the height of the inflow
θ' scale $\theta'_S = \tilde{\theta}'$, the mean θ' of the inflow
velocity scale $U_S = \tilde{U}$, velocity at the bottom of the inflow
time scale $T_S = H_S/U_S$.

(2) New choices for the dimensional scales are permitted when a stable layer is included in the domain. In these simulations the characteristics of the inflow of the density current can be altered by the action of a gravity wave moving backwards along the current. For this reason the dimensional scales are taken from the characteristics of the stable layer and not from those of the density current. Thus,

pressure scale $P_S = \Delta p_L$, pressure difference across stable layer
height scale $H_S = \Delta p_L/\rho_0 g$, height of the stable layer
θ' scale $\theta'_S = \theta''$, mean θ' in the stable layer
velocity scale $U_S = (-g(\theta''/\theta_0)H_S)^{1/2}$, the velocity of infinitesimal waves on the stable layer
time scale $T_S = H_S/U_S$.

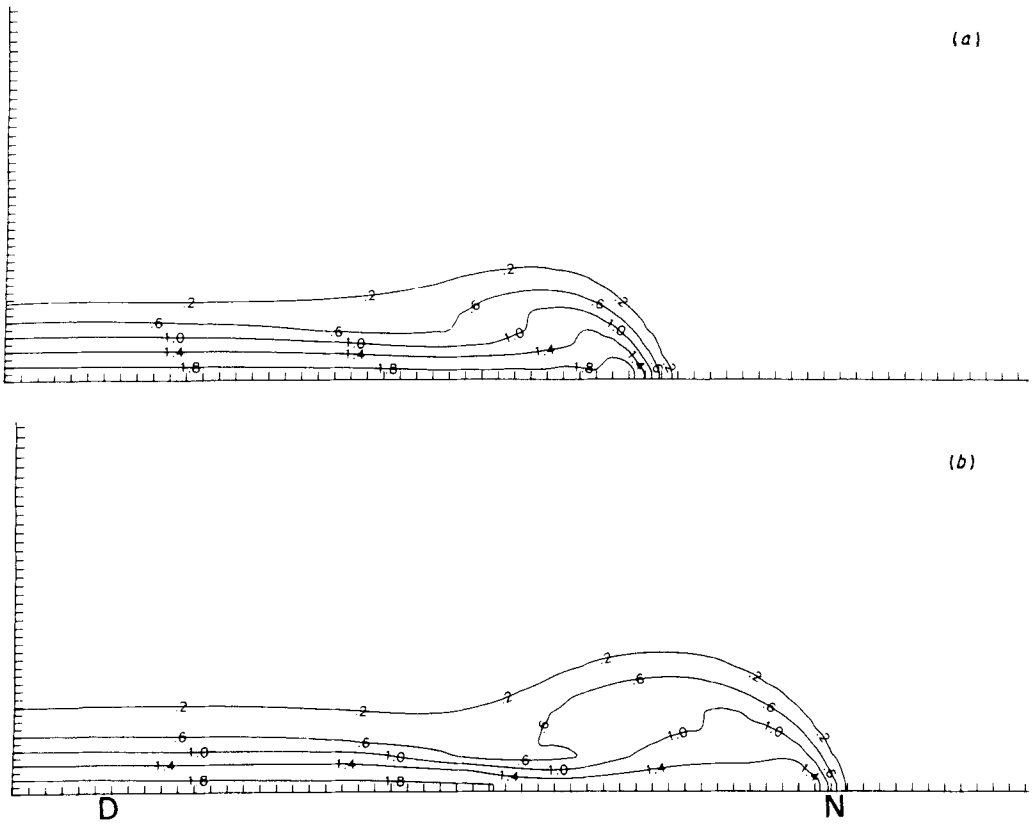

Figure 2. The potential temperature deviation θ' for a density current propagating into a neutral environment at two times: (a) $t = 48$; (b) $t = 96$.

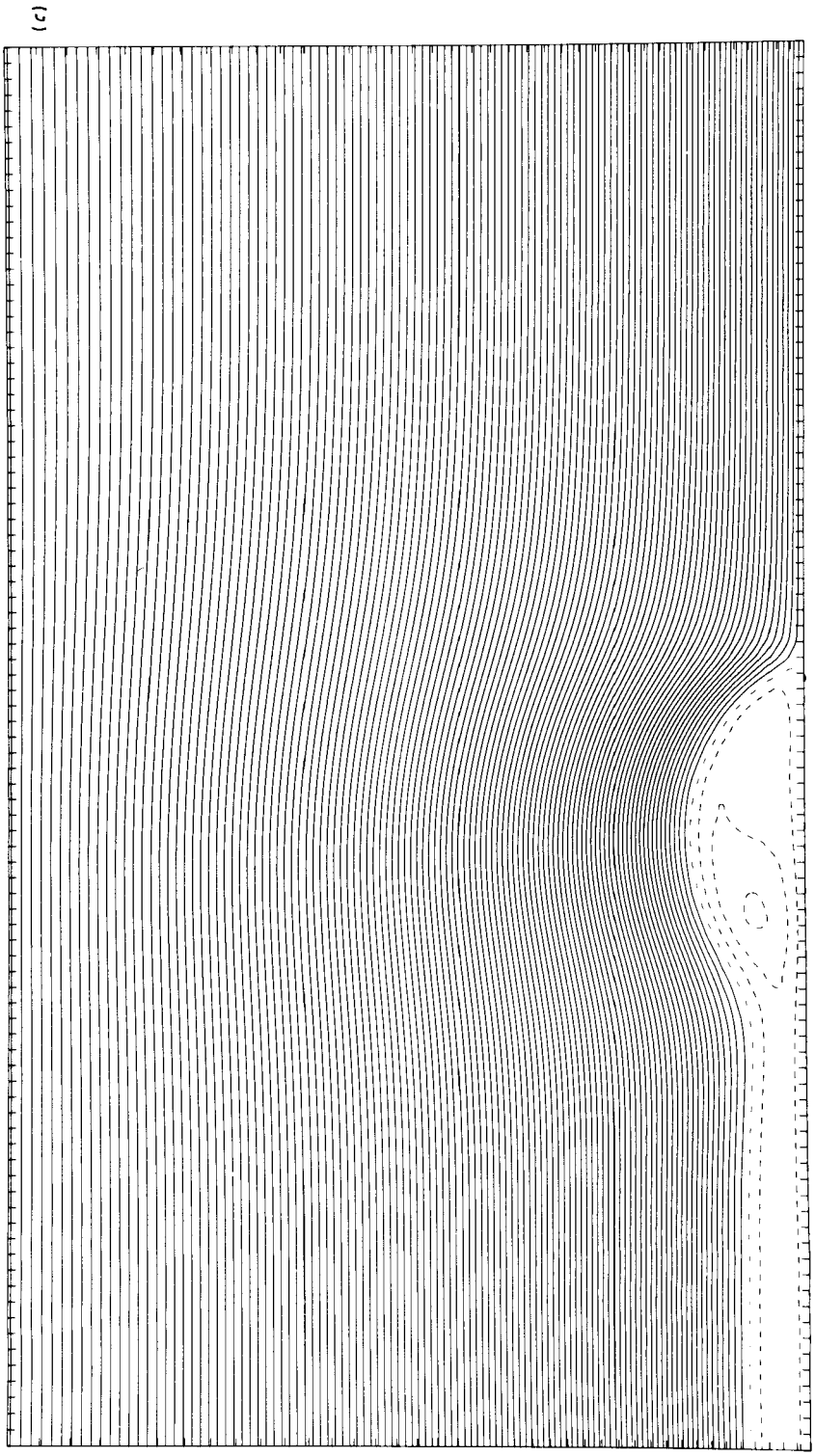

Figure 2(c). Streamfunction in a frame of reference in which the current is at rest, $t = 96$. The contour interval is 0·05 (non-dimensional units). The internal flow of the density current is shown by the negative contours (dashed lines).

3. Results

(a) *Simulation of a density current*

Before presenting the results from an undular bore simulation it is interesting to examine the performance of the model in simulating a density current in a neutral environment.

The model domain has 91 points in the horizontal and 40 in the vertical. The horizontal and vertical gridlengths are $\Delta x = 0{\cdot}5H_S$, $\Delta p = 0{\cdot}2P_S$ and the timestep $\Delta t = 0{\cdot}20T_S$. In the first simulation to be examined (experiment 1) $\tilde{\theta}'/\theta_0 = -0{\cdot}01$ and $\Delta p_I/\Delta p_T = \frac{1}{8}$ (see Fig. 1). Figure 2 shows the deviation potential temperature field at two simulation times $t = 48$ and $t = 96$ and the streamfunction at $t = 96$. In calculating the streamfunction a speed equal to the propagation speed of the density current is subtracted to bring the current's head to rest. As can be seen most of the observed features of density currents are reproduced in the simulation including the elevated head of the current and the flow towards the head at the ground and away from it above (Simpson 1969).

Three further experiments were carried out with different values for the total depth of the domain. Figure 3 shows the dependence of the propagation speed of the density current U_D on the total depth of the model.

In Fig. 3 the depth of the density current, D, is calculated in the following way. Firstly the integral of $\theta'(p)$ with height is determined from the model results and then equated to the integral that would result in a current with an assumed *step profile* of

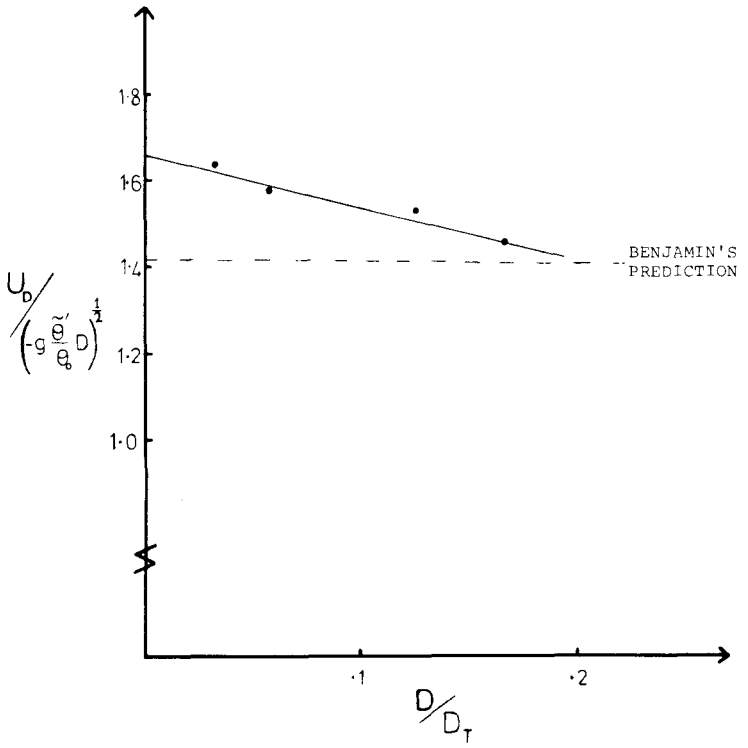

Figure 3. Density current velocity against the total depth of the domain for four experiments. Extrapolating the results in the limit $D_T/D \to \infty$ gives $U_D/\{(-g\tilde{\theta}'/\theta_0)D\}^{\frac{1}{2}} = 1{\cdot}65$, which is greater than the $\sqrt{2}$ predicted by Benjamin (1968).

$\theta'(p)$ of depth D and potential temperature deficit $\tilde{\theta}'$. This method of analysis is justified by the fact that the driving force of the current is the hydrostatic pressure difference which depends only on the integral of potential temperature deficit (see Benjamin 1968). Benjamin showed that when a density current moves into an infinite expanse of fluid, energy must be lost. However, using Bernouilli's equation around a circuit which avoided the turbulent head of the current, Benjamin was able to show that the ratio $U_D/\{-g(\tilde{\theta}'/\theta_0)D\}^{\frac{1}{2}}$, for a current in an infinite expanse of fluid, should be $\sqrt{2}$ (D is some mean depth in the turbulent wake region of the current). As can be seen from Fig. 3 all of the ratios measured have a value greater than $\sqrt{2}$. Furthermore, a linear extrapolation back to $D/D_T = 0{\cdot}0$ (the case examined by Benjamin) gives a ratio of 1·65; thus for a given pressure difference the current travels approximately 16% faster than predicted. This, at first curious result, is due to the fact that Benjamin ignored the internal flow of the density current by setting the pressure far downstream (point D in Fig. 2(b)) equal to that at the nose (point N), whereas in fact the pressure is slightly greater at the nose. Thus the pressure difference between the nose of the current and points far upstream is *greater* than that predicted by Benjamin (since the difference in pressure between points far upstream and D, which depends on the hydrostatic pressure difference only, remains constant for a given density current). Thus, a density current with an internal flow is able to propagate faster than a current without such a flow.

It should be noted that Britter and Simpson (1978) have included the internal flow of a density current in a semi-empirical analysis. They calculate several Froude numbers based on different velocity and length scales in the flow. However, the scales that they use cannot be related directly to the hydrostatic pressure difference, and thus it is difficult to make comparison with the present work.

(*b*) *Density current and stable layer* (*step profile*)

In the previous section the influence of a density current on an ambient neutral environment was considered. When a stable layer is included the density current is able to modify far ahead the environment into which it moves.

The simulation (experiment 2) to be examined has a step profile in $\theta'(p)$ and the following values for the main parameters:

$$\theta''/\theta_0 = -0{\cdot}01 \qquad \Delta p_L/\Delta p_T = 0{\cdot}125$$

$$\tilde{\theta}'/\theta_0 = -0{\cdot}075 \qquad \Delta p_I/\Delta p_T = 0{\cdot}075$$

$$\Delta x = 1{\cdot}2H_S \qquad \Delta p = 0{\cdot}2P_S \qquad \Delta t = 0{\cdot}3T_S$$

recalling that the dimensional scales are now taken from the stable layer. The domain has 145 points in the horizontal and 40 in the vertical.

Since the timescale for development of the undular bore is greater than the time taken for the bore to cross the domain, a Galilean transformation is applied early in the simulation to keep the bore inside the model domain. In all of the following simulations the opposing velocity was applied just after cooling of the stable layer and had a value of $-0{\cdot}9$. Figure 4 shows the deviation potential temperature field at $t = 250$ and $t = 420$ and the streamfunction of the flow at $t = 420$ in a frame of reference in which the bore is at rest. As can be seen the stable layer is progressively smeared out as it moves from right to left. This smearing is caused by the vertical smoothing term in the potential temperature equation, which is included partly to counteract numerical dispersion but also as a representation, albeit crude, of turbulent mixing.

In Figs. 4(a) and (b) the nose of the density current can be identified as the point where the isotherms intersect the lower boundary. It is clear therefore that a disturbance

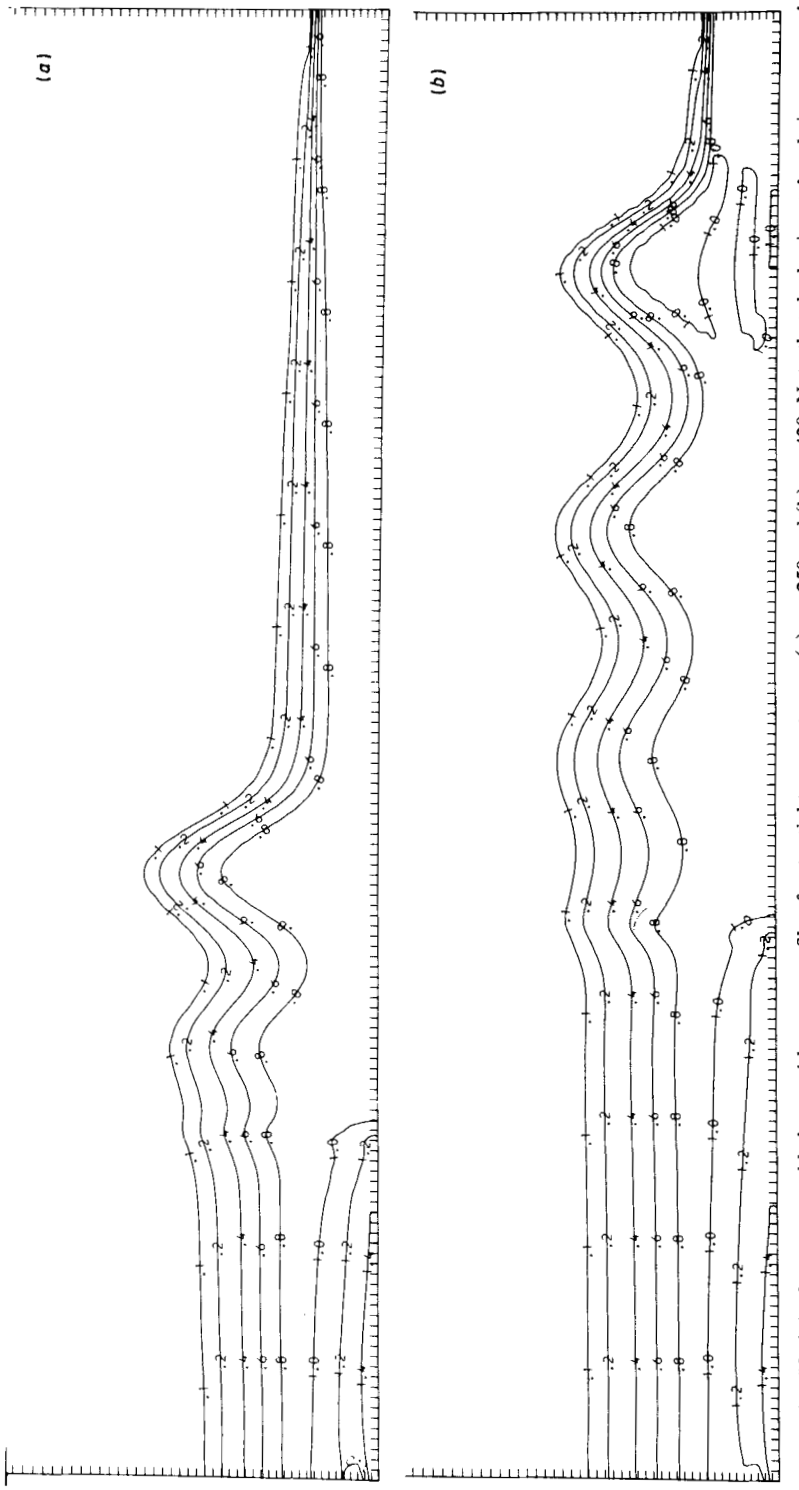

Figure 4. Undular bore on a stable layer with a step profile of potential temperature at (a) $t = 250$ and (b) $t = 420$. Note that the horizontal scale is contracted by a factor of 3·8 relative to Fig. 2. The density current can be seen in the lower left hand corner of the domain. The closed isotherms in the leading crest in (b) are caused by numerical dispersion which results when the sharp gradients of potential temperature are advected upwards.

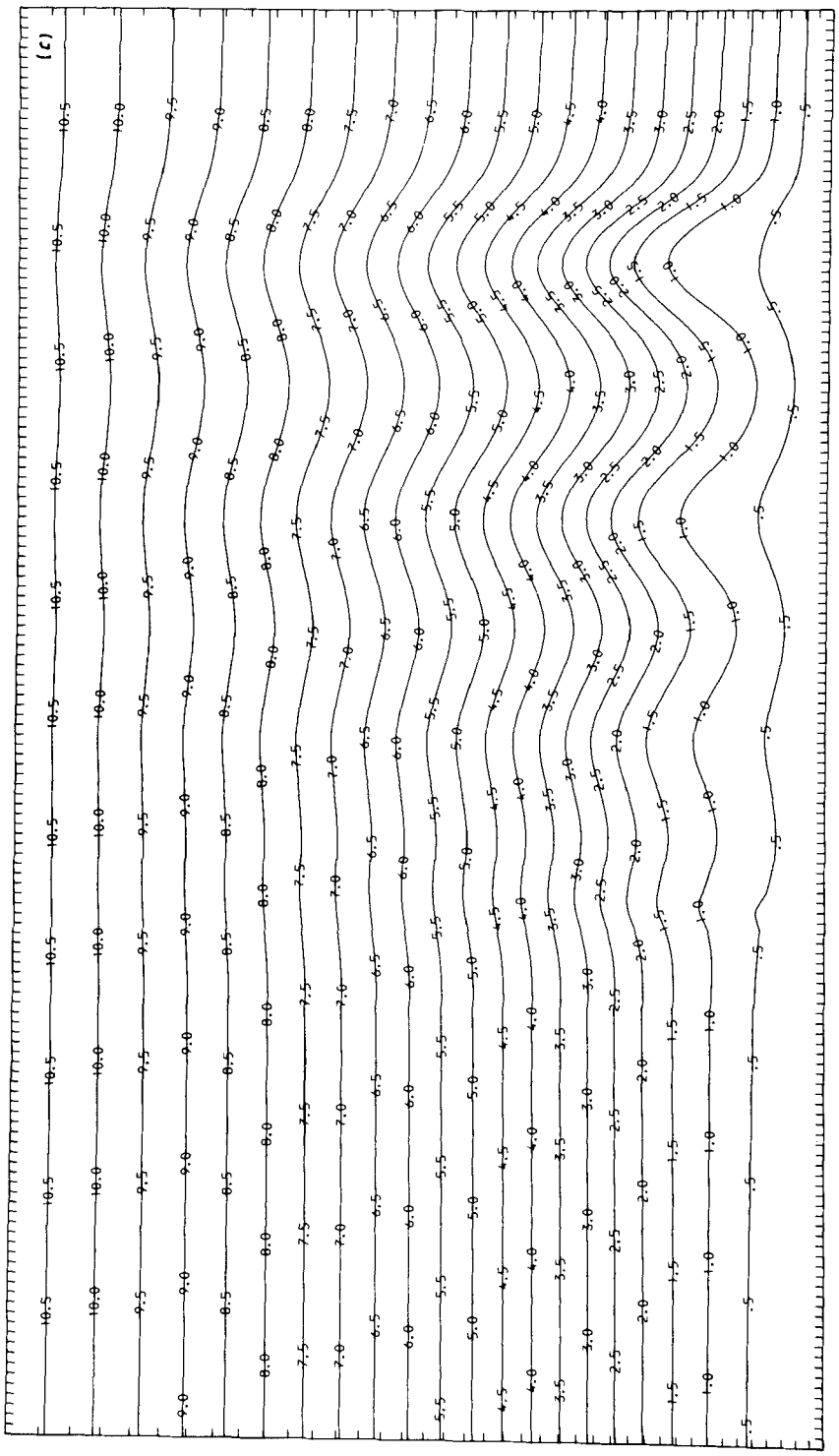

Figure 4(c). Streamlines for the flow in a frame of reference in which the bore is at rest at $t = 420$.

has moved ahead of the density current. That this disturbance is indeed an undular bore is shown in the increase of the mean depth of the stable layer and consequently in the increase of the mean surface pressure. Furthermore the development of the bore follows a pattern similar to that observed in the laboratory experiments with waves forming above the density current and then moving ahead of it. By the end of the simulation three such waves have moved ahead of the current.

To compare the speed of the bore with theory it is necessary to include in the existing analytic models the effect of a top boundary. For an infinite incompressible fluid the speed of a bore U_B of mean downstream depth d moving into a layer of depth D_L is given by,

$$U_B^2/(g' D_L) = (d/2D_L)(1 + d/D_L) = F \tag{3}$$

where $g' = (\rho'/\rho_0)g$ (see for example Turner 1973). The same results follow for a compressible system with the exception that ρ'/ρ_0 is replaced by $-\theta'/\theta_0$ and height differences by pressure differences.

If the fluid is deep but not of infinite extent then it is straightforward to show that the speed of the bore is given by

$$U_B^2/(g' D_L) = F(1 - FD_L/D_T) \tag{4}$$

for $D_L/D_T \ll 1$, where F is the same as before and D_T is the total depth.

To evaluate d, a mean depth is calculated in the same way as for the depth of the density current and then averaged over one wavelength. This averaging is carried out

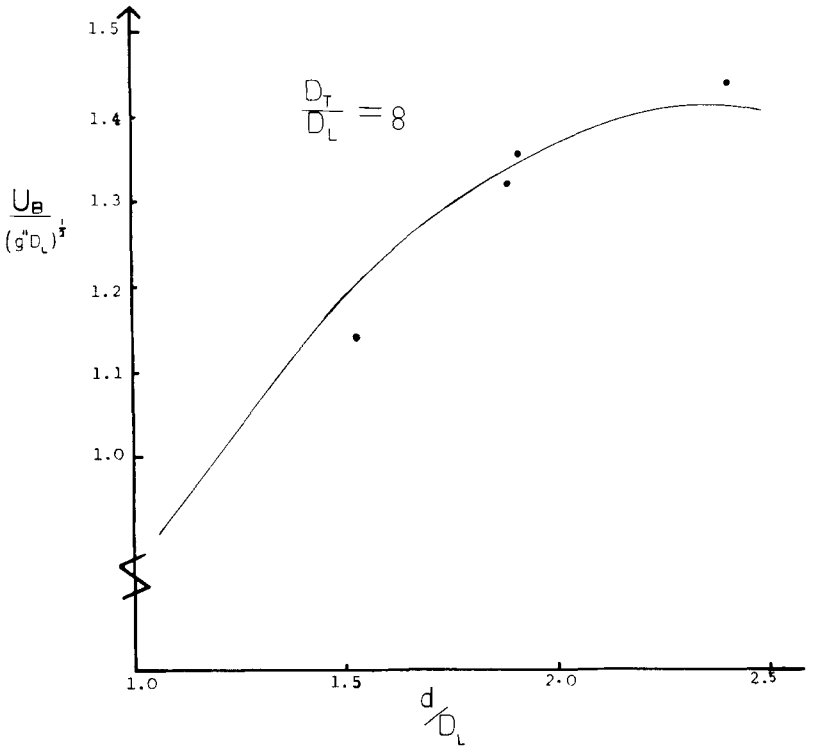

Figure 5. Speed of the bore against its depth for four simulations. The continuous line is the prediction of irrotational theory, Eq. (4).

as far from the leading edge of the bore as possible where the wave amplitude is small. As noted by Wilkinson and Bannon (1977) the equations for an undular bore should include a term involving the wave stress. However, the contribution of this term is small and is minimized by averaging in the region where the wave amplitude is least.

Applying the above analysis to the bore in Fig. 4 a depth d is obtained of $1{\cdot}93D_L$. Substituting this into Eq. (4) and using $D_L/D_T = \frac{1}{8}$ we obtain $U_B/(g''D_L)^{\frac{1}{2}} = 1{\cdot}35$ where $g'' = -(\theta''/\theta_0)g$.

In the numerical model the simulated bore moves at a speed U_B given by $U_B/(g''D_L)^{\frac{1}{2}} = 1{\cdot}32 \pm 0{\cdot}04$, where the error bounds give an indication of the non-constancy of the bore's velocity. As can be seen the degree of agreement between numerical and analytic model is very good. The above analysis has been carried out on a number of bores of differing strength and the results plotted in Fig. 5.

So far the bore has been examined in isolation. To determine if the depth of the bore produced agrees with the strength of the density current, the analytic model developed in Crook (1983) can be applied. The model uses the basic equations for a density current in a two-layer fluid (Holyer and Huppert 1980) but includes the possibility of a bore running ahead of the density current. Briefly, equation 2·12 of Holyer and Huppert, which describes the flow in the vicinity of the density current, is used and Eq. (4) of the present study for the flow through the bore. The two flows are linked by a suitable continuity equation and then for a given density current the speed of the bore produced can be calculated.

It was originally felt that as long as the mass flux of the density current before it entered the stable layer was known, then the strength of the bore could be determined. However, when the current meets the stable layer large gravity waves not only move ahead of the density current but also propagate backwards along the current. These gravity waves can effect a change in the current's mass flux. Thus, there is no guarantee that the mass flux of the current is the same after it enters the stable layer as it was before.

However, the analytical model can be used to determine if the strength of the bore produced agrees with the velocity of the density current *after* it has moved into the stable layer and pushed waves ahead of itself.

In experiment 2 the average potential temperature deficit of the density current, *after* the waves have moved ahead, is $\theta_N'/\theta_0 = -0{\cdot}0126$ and that of the stable layer $\theta'/\theta_0 = -0{\cdot}010$. Thus the parameter $\gamma\ (=\theta_N'/\theta'' - 1)$ in Holyer and Huppert is equal to 0·26. The velocity of the density current, *after* the waves have moved ahead, is $U_D = 1{\cdot}04$. Solving the system of equations the following parameters are determined: $d = 1{\cdot}99$ and $U_B = 1{\cdot}37$, which are to be compared with $d = 1{\cdot}93$ and $U_B = 1{\cdot}32 \pm 0{\cdot}04$ from the numerical model.

As can be seen the analytical model slightly overestimates the depth and speed of the bore. Nevertheless, the level of agreement is encouraging when it is considered that the analytical model assumes irrotational flow and a homogeneous density current.

The above method of analysis has been performed for two further simulations, and the results compared with the analytical model in Table 1.

TABLE 1. COMPARISON BETWEEN NUMERICAL RESULTS AND THE ANALYTICAL MODEL OF CROOK (1983)

U_D	γ	d(calc.)	d(num. model)
1·07	0·20	2·11	1·94
0·97	0·14	2·02	1·88

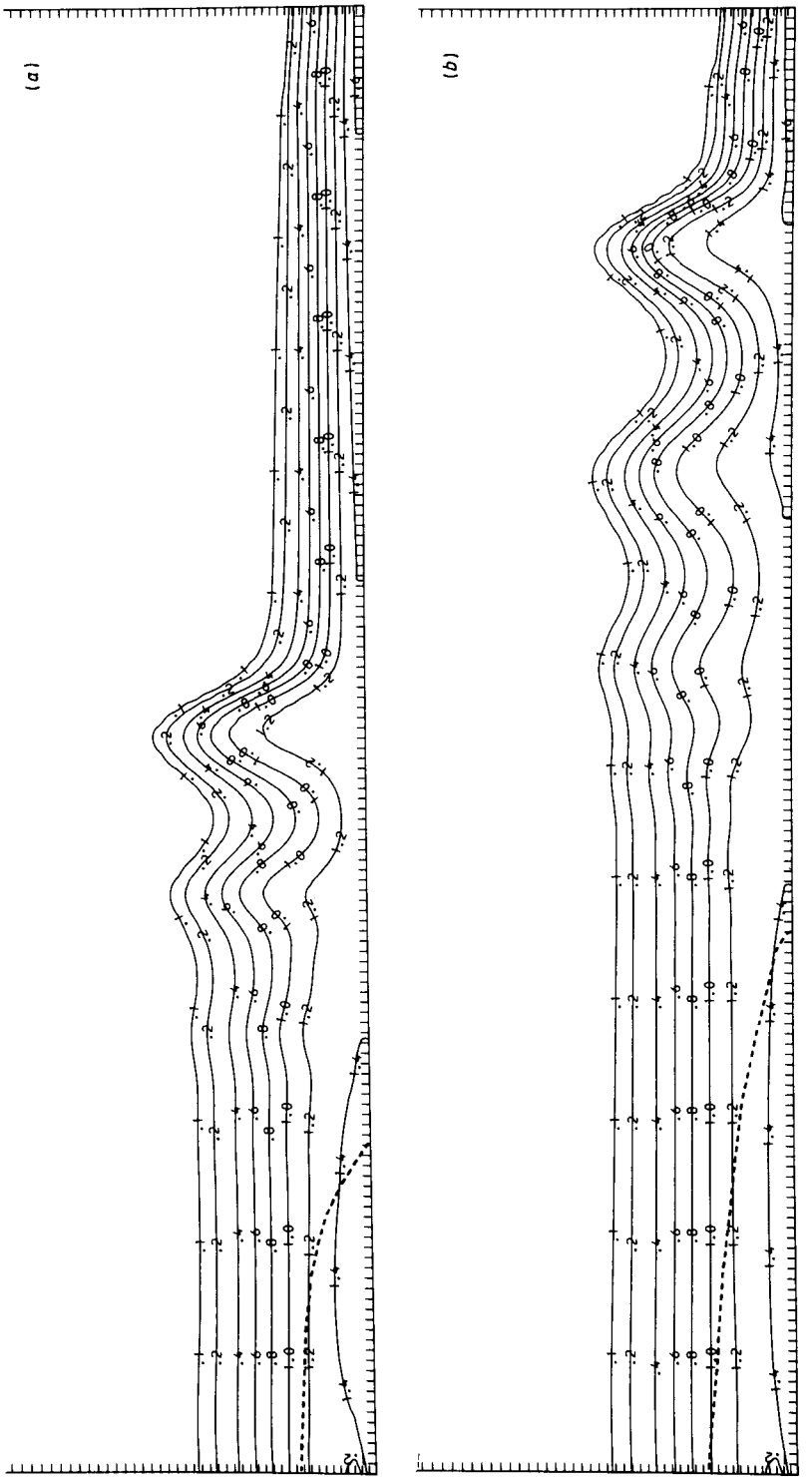

Figure 6. Undular bore on a linear stable layer at (a) $t = 250$ and (b) $t = 350$. The position of the density current is indicated by a tracer fluid injected at inflow. The 0·1 contour of this tracer (indicating fluid with a concentration of 10% of the maximum injected) is shown by the dashed line.

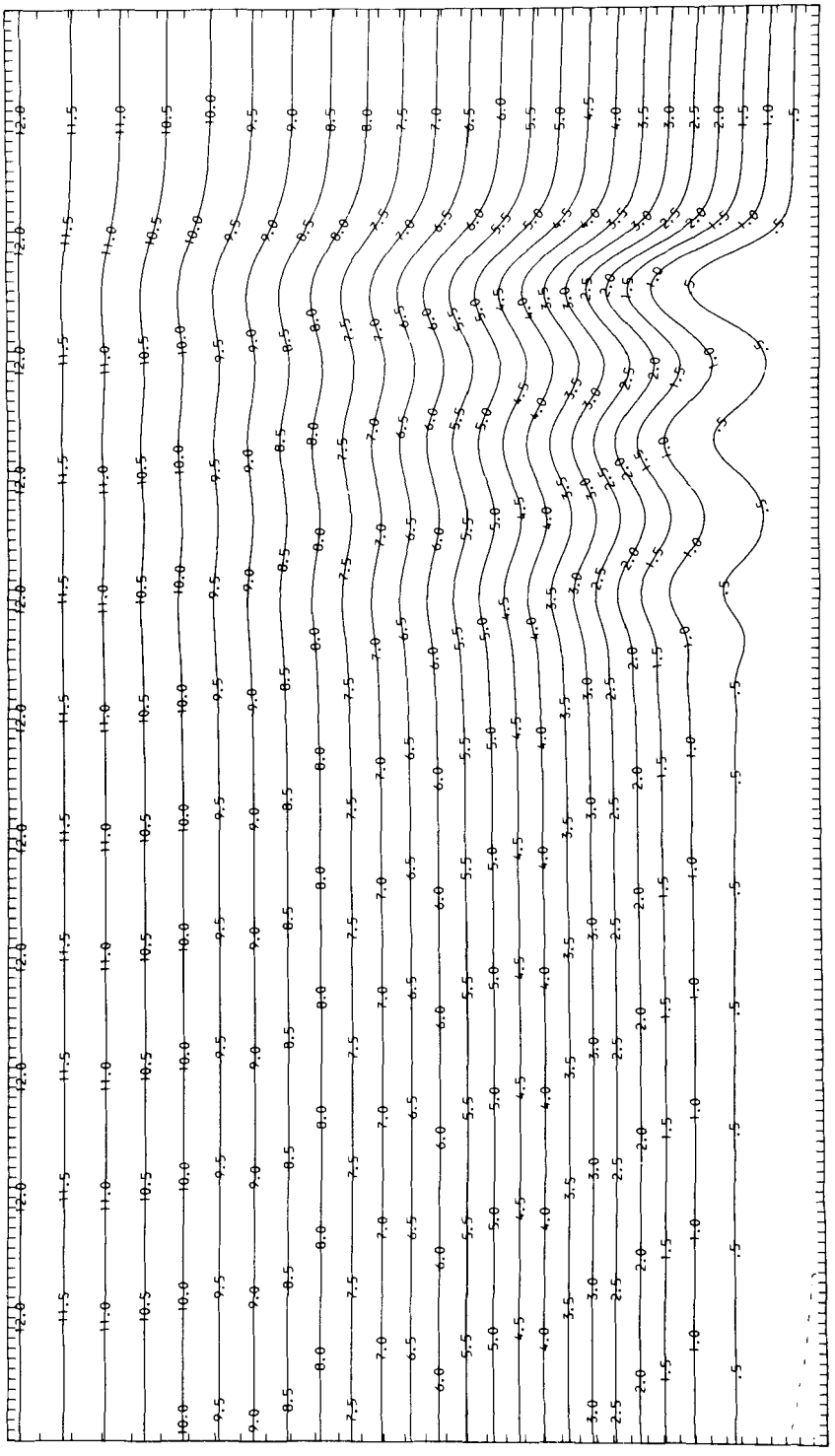

Figure 7. Streamfunction, at $t = 370$ minutes, for an undular bore with a similar strength to the morning glory observed on 4 October 1979. To be compared with Clarke *et al.* (1981) Fig. 13.

(c) *Stable layer with a linear profile of $\theta'(p)$*

A step profile for the potential temperature in the stable layer, although facilitating comparison with analytic models, does not bear a close resemblance to the atmosphere. A more realistic profile and that observed on the morning glory expeditions (see Clarke *et al.* 1981) is a linear change of potential temperature in the stable layer.

The numerical model was run with the same density current parameters as in experiment 2 but with a stable layer with a linear profile of $\theta'(p)$ and a mean value of $\theta''/\theta_0 = -0{\cdot}01$. This simulation will be called experiment 3. The potential temperature fields at $t = 250$ and $t = 350$ are shown in Figs. 6(a) and (b). Since the potential temperature of the current is now no longer the lowest in the flow it is difficult to use it to define the position of the current. For this reason an additional variable is included: that of an inert tracer injected at the inflow of the density current. The 10% contour of this tracer fluid is indicated by the dashed lines in Fig. 6.

One difference to note between experiments 2 and 3 is that the undulations in the latter experiment decay much more rapidly. For a bore on a step layer it is well known that energy must be lost downstream (see Turner 1973) and that in an undular bore this is accomplished by wave radiation. However, as shown in appendix B, an energy-conserving solution can be found for a bore on a 'linear' stable layer. Hence energy radiation is not required, and so the waves evanesce in the horizontal.

It is interesting to compare the results from the numerical model with some of the measurements of the morning glory. The glory of 4 October 1979 will be used for comparison (Clark *et al.* 1981) since it is the best documented so far.

The stable layer on that day had a depth of 630 m and a mean potential temperature deviation θ'' of -4°C corresponding to a Brunt–Väisälä period of 5·1 minutes. A numerical simulation was chosen that produced a bore of approximately the same strength as on 4 October (where strength is defined as the pressure across the bore, ~0·8 mb for the glory of that day). The wavelength and velocity for the simulated and observed bores are compared in Table 2.

TABLE 2. COMPARISON BETWEEN NUMERICAL RESULTS AND THE MORNING GLORY OF 4 OCTOBER 1979

	Numerical model	Observed morning glory
Distance between 1st and 2nd crest	11·1 km	10·0 km
Velocity	10·9 m s^{-1}	11·2 m s^{-1}

In Fig. 7 the streamlines for the flow through the bore at $t = 370$ minutes are plotted. An opposing velocity has been applied to bring the bore to rest. When this is compared with Fig. 13 of Clarke *et al.* the similarity in structure between the modelled and observed bores is quite evident. However, one discrepancy is that the closed streamlines that were observed on 4 October do not appear in the numerical simulations. However, the forward velocity in the leading wave increases monotonically and is in fact 90% of the speed of the bore at the end of the simulation, which suggests that a closed circulation might develop if the model was run for a longer time. If this is the case then any fluid that is advected with the bore could not have come from far downstream but is 'picked up' by the bore as it passes. This is supported by the fact that none of the tracer fluid in the density current can be seen in the bore in Fig. 6(b).

4. Concluding remarks

In the preceding simulations the fluid above the stable layer has been unstratified. This means that energy in the bore is trapped in the stable layer and cannot propagate away as it would in the real atmosphere. Nevertheless encouraging agreement has been found between the model results and the observed features of the morning glory.

The model has been run with a stratified upper layer and the results will be reported fully in a later paper. Briefly though, if the ambient environment is unsheared, an internal gravity wave trapped by the upper and lower surfaces moves ahead of the density current and little or no disturbance appears on the stable layer. This behaviour occurs even when the very low values of static stability observed at Burketown ($B = 5{\cdot}0\times10^{-6}\mathrm{m}^{-1}$) are used. However, if the ambient environment is sheared in such a way that the flow at upper levels opposes, increasingly, the motion of the density current then this large-scale gravity wave becomes evanescent in the vertical and does not propagate ahead of the current. A disturbance at low levels does however move ahead and this shows many similarities to the observed structure of the morning glory. This behaviour agrees with the theory developed by Scorer (1949) which states that for energy to be trapped at low levels the Scorer parameter $l^2 = gB/(U-c)^2 - U''/(U-c)$, where c is the wavespeed, must decrease sufficiently rapidly with height. It is also consistent with climatic data for the northern Queensland region which show that a strong westerly jet (i.e. in the sense to oppose glorys moving from the east) centred about 600 mb develops in mid-winter and remains until about November which is the same period as that of maximum frequency of morning glorys (Clarke *et al.* 1981).

Appendix A

The continuity equation in the model is of the form

$$\partial u/\partial x + \partial \omega/\partial p = 0 \tag{A1}$$

where ω is the total rate of change of pressure. If this equation is integrated over the semi-infinite domain $0 \leq x \leq x_\infty$ (where $x_\infty \to \infty$) then the following relation is obtained

$$\int_{p_{TOP}}^{p_0} u(0)\,dp - \int_{p_{TOP}}^{p_0} u(x_\infty)\,dp = 0 \tag{A2}$$

where the boundary conditions $\omega = 0$ at $p = p_{TOP}, p_0$ have been used. If at the commencement of the simulation the velocity $u(x,p)$ is identically zero throughout the domain and the flow is only perturbed in the vicinity of $x = 0$ then $u(x,p)$ must remain zero at $x = x_\infty$ for all finite time. Therefore from Eq. (A2)

$$\int_{p_{TOP}}^{p_0} u(0)\,dp = 0 \tag{A3}$$

for all time. To ensure that Eq. (A3) is satisfied, a relation between the pressure at the lateral boundaries and the velocity field must hold. This relation can be found by integrating the horizontal momentum equation,

$$\partial u/\partial t = -g\partial h'/\partial x + D \tag{A4}$$

where D includes advective and smoothing terms. Integrating over the domain of the model the following equation is obtained,

$$\int_{p_{TOP}}^{p_0} gh'(x_\infty)\,dp - \int_{p_{TOP}}^{p_0} gh'(0)\,dp = \int_{p_{TOP}}^{p_0}\int_0^{x_\infty} D\,dx\,dp - \frac{\partial}{\partial t}\int_{p_{TOP}}^{P_0}\int_0^{x_\infty} u\,dx\,dp \qquad \text{(A5)}$$

or in finite difference form,

$$\sum_{p_{TOP}}^{p_0} gh''(x_\infty)\Delta p - \sum_{p_{TOP}}^{p_0} gh''(0)\Delta p = \sum_0^{x_\infty}\sum_{p_{TOP}}^{p_0} D^{t-\Delta t}\Delta p\,\Delta x - \left(\sum_0^{x_\infty}\sum_{p_{TOP}}^{p_0} u^t(x,p) - \sum_0^{x_\infty}\sum_{p_{TOP}}^{p_0} u^{t-\Delta t}\right)\frac{\Delta x\,\Delta p}{\Delta t} \qquad \text{(A6)}$$

where an explicit representation of the time derivative has been used.

As shown previously from the continuity equation, $\sum_{p_{TOP}}^{p_0} u(x,p) = F$ where F is a constant in x. Therefore Eq. (A6) can be written

$$\sum_{p_{TOP}}^{p_0} gh''(x_\infty)\Delta p - \sum_{p_{TOP}}^{p_0} gh''(0)\Delta p = \sum\sum D^{t-\Delta t}\Delta p\,\Delta x - \frac{L\Delta x\Delta p}{\Delta t}(F^t - F^{t-\Delta t}) \qquad \text{(A7)}$$

where L is the number of gridpoints in the horizontal.

Now F^t can be set as the vertically integrated velocity at the start of the simulation and hence all of the quantities on the right-hand side of Eq. (A7) are known at time $t - \Delta t$. Equation (A7) is therefore a relation that the height field at the lateral boundaries at time t must satisfy if the vertically integrated velocity is to remain constant.

In the numerical simulation Eq. (A7) is implemented in the following way. At each timestep boundary values for h' are calculated from radiation conditions and then a correction, $\Delta h'$, constant with height calculated from Eq. (A7) is added at one end. When this is done the integrated velocity is kept constant to within rounding error.

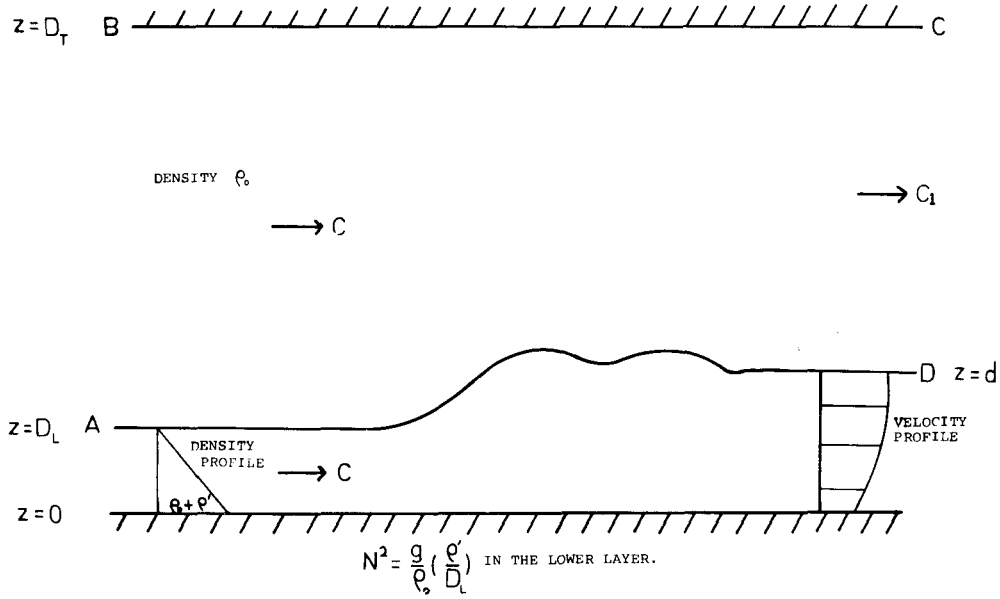

Figure 8. Undular bore on a linear stable layer.

APPENDIX B

The system to be examined is shown in Fig. 8. If the flow is incompressible then a streamfunction η can be defined such that

$$u = c\partial\eta/\partial z \qquad w = -c\partial\eta/\partial x \tag{B1}$$

where c is the constant upstream velocity. Hence far upstream $\eta = z$.

Now for an energy-conserving solution the total head $H = p + \frac{1}{2}\rho u^2 + \rho gz$ is constant along a streamline. When this condition and the Boussinesq approximation is applied it can be shown (see Long 1953) that

$$\nabla^2\eta' + K^2\eta' = 0 \qquad K^2 = N^2/c^2 \tag{B2}$$

where η' is the deviation of a streamline from its upstream position.

If the flow is assumed horizontal far downstream, then $\eta_x = 0$ so that Eq. (B2) becomes

$$\partial^2\eta'/\partial z^2 + K^2\eta' = 0 \tag{B3}$$

which has the solution $\eta' = A\sin Kz + B\cos Kz$, therefore

$$\eta = z + A\sin Kz + B\cos Kz.$$

As there is a continuous streamline along the bottom of the flow $B = 0$. Similarly at the top of the stable layer far downstream ($z = d$) $\eta = D_L$. Therefore

$$A = (D_L - d)/\sin(Kd).$$

To close the system continuity of pressure across the interface must be used. If $p \equiv 0$ far upstream at the interface then Bernoulli's equation along the streamline A $\rightarrow$ D gives

$$\begin{aligned} \tfrac{1}{2}c^2 + gD_L &= p_D/\rho_0 + \tfrac{1}{2}c^2\{(\partial\eta/\partial z)_{z=d}\}^2 + gd \\ p_D/\rho_0 &= g(D_L - d) + \tfrac{1}{2}c^2[1 - \{1 + (D_L - d)K\cot Kd\}^2]. \end{aligned} \tag{B4}$$

From the circuit A $\rightarrow$ B $\rightarrow$ C $\rightarrow$ D,

$$p_D/\rho_0 = g(D_L - d) + \tfrac{1}{2}(c^2 - c_1^2). \tag{B5}$$

Equating pressure across the interface gives

$$(c_1 - c)/c = (D_L - d)K\cot Kd. \tag{B6}$$

Now if $D_T \rightarrow \infty$, $c_1 \rightarrow c$ by continuity, therefore $\cot(Kd) = 0$, which has the solution $Kd = (2n + 1)\pi/2$, $n = 0, 1, 2, 3, \ldots$.

Thus the fastest moving bore which conserves energy has a velocity $c = 2Nd/\pi$.

ACKNOWLEDGMENTS

This work forms part of a thesis submitted by the first author for degree of Ph.D. at the University of London. This author is grateful to the British Council for the receipt of a Commonwealth Scholarship.

References

Benjamin, T. B.	1968	Gravity currents and related phenomena. *J. Fluid Mech.*, **31,** 209–248
Britter, R. E. and Simpson, J. E.	1978	Experiments on the dynamics of a gravity current head. *ibid.*, **88,** 223–240
Clarke, R. H.	1972	The Morning Glory: an atmospheric hydraulic jump. *J. Appl. Meteor.*, **11,** 304–311
Clarke, R. H., Smith, R. K. and Reid, D. G.	1981	The Morning Glory of the Gulf of Carpentaria: An atmospheric undular bore. *Mon. Wea. Rev.*, **109,** 1733–1750
Crook, N. A.	1983	Pp. 349–353 in *The formation of the Morning Glory. Mesoscale Meteorology–Theories, Observations and Models.* D. K. Lilly and T. Gal-Chen (Eds.), D. Riedel
	1984	'A Numerical and Analytical Study of Atmospheric Undular Bores'. Ph.D. Thesis, University of London
Holyer, J. Y. and Huppert, E. H.	1980	Gravity currents entering a two-layer fluid. *J. Fluid. Mech.*, **100,** 739–767
Kirk, T. H.	1961	"Pressure Jumps" at Malta. *Met. Mag.*, **90,** 206–209
Long, R. R.	1955	Some aspects of the flow of stratified fluids. A theoretical investigation. *Tellus*, **5,** 42–57
Maxworthy, T.	1980	On the formation of nonlinear internal waves from the gravitational collapse of mixed regions in two and three dimensions. *J. Fluid Mech.*, **96,** 47–64
Miller, M. J. and Pearce, R. P.	1974	A three-dimensional primitive equation model of cumulonimbus convection. *Quart. J. R. Met. Soc.*, **100,** 133–154
Miller, M. J. and Thorpe, A. J.	1981	Radiation conditions for the lateral boundaries of limited-area models. *ibid*, **107,** 615–628
Moncrieff, M. W. and Miller, M. J.	1976	The dynamics and simulation of tropical cumulonimbus and squall lines. *ibid*, **102,** 373–394
Scorer, R. S.	1949	Theory of waves in the lee of mountains. *ibid*, **75,** 41–56
Shreffler, J. H. and Binkowski, F. S.	1981	Observations of pressure jump lines in the Midwest. *Mon. Wea. Rev.*, **109,** 1713–1725
Simpson, J. E.	1969	A comparison between laboratory and atmospheric density currents. *Quart. J. R. Met. Soc.*, **95,** 758–765
	1982	Gravity currents in the laboratory, atmosphere and ocean. *Ann. Rev. Fluid Mech.*, 213–234
Smith, R. K., Crook, N. and Roff, G.	1982	The Morning Glory: an extraordinary atmospheric undular bore. *Quart. J. R. Met. Soc.*, **108,** 937–956
Turner, J. S.	1973	*Buoyancy effects in fluids.* Cambridge University Press
Wilkinson, D. L. and Bannon, M. L.	1977	'Undular Bores'. Sixth Australasian Hydraulics Conference, 369–373